論 文 の 内 容 の 要 旨

応用生命工学専攻
平成 28 年度博士課程入学
氏　　名　　王　　翌霞
指導教員名　　野尻　秀昭

論文題目

Structural insight into the mechanism of angular dioxygenation in carbazole 1,9a-dioxygenase

（カルバゾール 1, 9a−ジオキシゲナーゼにおける核間二水酸化反応の構造基盤）

Introduction

Carbazole (CAR) is a recalcitrant *N*-heterocyclic aromatic compound with mutagenicity and toxicity that is predominant in coal tar creosote, the release of which has caused environmental concerns. To achieve bioremediation of CAR in the environment, various CAR-degrading bacteria that use CAR as the sole source of nitrogen, carbon and energy, have been isolated from diverse niches and the corresponding catabolic gene (*car*) clusters from these bacteria have also been identified and characterized. It has been reported that angular dioxygenation of CAR, adding two hydroxyl groups with *cis*-confirmation to the angular position (C9a) carbon bound to the imino nitrogen and its adjacent C1 carbon, is most important by destroying the planar structure from which the toxicity derives, resulting in complete mineralization of CAR. Carbazole 1,9a-dioxygenase (CARDO), a member of three-component Rieske non-heme iron oxygenase (RO) consisting of ferredoxin reductase (Red, 37 kDa), ferredoxin (Fd, 13 kDa) and homo-trimeric terminal oxygenase (Oxy, 132 kDa), has been reported to initiate the degradation of CAR by angular dioxygenation to yield unstable *cis*-dihydrodiol, which subsequently converts to 2'-aminobiphenyl-2,3-diol (ABP-diol) spontaneously. To illuminate the mechanism of angular dioxygenation in CARDO, catalytic cycle of CARDO has been proposed on the basis of various well-determined structures of CARDO and other ROs (Fig. 1). As is shown in Fig. 1, $Oxy_{ox/red}$ (1) in resting state contains oxidized Rieske cluster and reduced mononuclear iron in each subunit. Then reduced Fd (Fd_{red}) binds to the resting Oxy to form the transient complex of $Oxy_{ox/red}$:Fd_{red}. One electron is transferred from Fd_{red} to $Oxy_{ox/red}$, resulting in the changes of redox state of both Oxy and Fd to for the complex of $Oxy_{red/red}$:Fd_{ox} (2), followed by the release of oxidized Fd (Fd_{ox}). The $Oxy_{red/red}$ (3) then are able to bind with substrate and oxygen to initiate the dioxygenation of substrate. According to the possible binding sequence of substrate and oxygen, two pathways have been proposed: in pathway 1, aromatic substrate (eg. CAR) is available to the non-heme iron prior to oxygen molecule to form the binary $Oxy_{red/red}$:CAR (4a); in pathway 2, oxygen molecule binds to the active site ahead of substrate, resulting in the formation of $Oxy_{ox/ox}$:O_2 (4b). When both substrate and O_2 are available to the active site, substrate transformation starts ($Oxy_{ox/ox}$:CAR:O_2, (5)). The finally generated *cis*-dihydrodiol product binds at the active site with both oxygen atoms coordinated to the ferric iron ($Oxy_{ox/ox}$:ABP-diol, (6)). The active site of $Oxy_{ox/ox}$:ABP-diol is reduced by receiving the second electron from Fd_{red} to form the complex of $Oxy_{ox/red}$:Fd_{ox}:ABP-diol binding with protonated ABP-diol (7). Two possible pathways have also been proposed based on the presumed release order of Fd_{ox} and product: in pathway 3, Fd_{ox} dissociates from the complex before the release of product ($Oxy_{ox/red}$:ABP-diol, (8a)); in pathway 4, ABP-diol

escapes from the active site before the dissociation of $Oxy_{ox/red}$:Fd_{ox} complex (8b). Finally the Oxy returns to the resting state and initiates next turnover. To date, the structures of $Oxy_{ox/red}$ (1), $Oxy_{red/red}$:Fd_{ox} (2), $Oxy_{red/red}$ (3), $Oxy_{ox/red}$:Fd_{ox} (8b), as well as Fd in resting and reduced states (Fd_{ox} and Fd_{red} in Fig. 1), have been solved. The current study continues on determining the structures of CARDO in substrate binding, O_2 activation, product formation and release to illustrate the mechanism of angular dioxygenation in CARDO from structural insight.

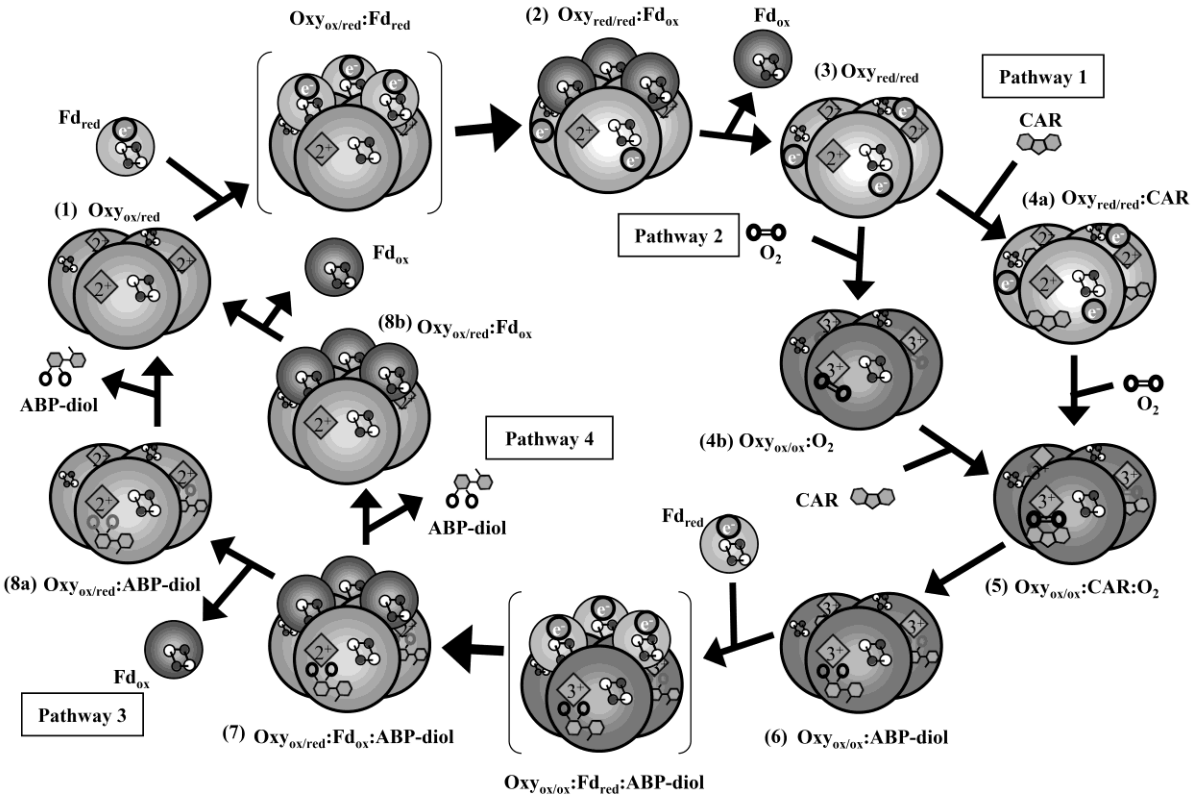

Fig. 1 Proposed catalytic cycle of angular dioxygenation in CARDO. The subscripts "ox" and "red" refer to the oxidized and reduced states of redox centers (in order of Rieske cluster/non-heme iron), respectively. e^-: electron.

Chapter 2. Substrate binding and product formation in Oxy of CARDO

In pathway 1, substrate binding was achieved by soaking crystals of previously obtained $Oxy_{red/red}$ (3) in dimethyl sulfoxide (DMSO) solution of CAR under anaerobic condition. The crystal structure of $Oxy_{red/red}$:CAR (4a) was determined at 2.2 Å resolution in Photon Factory (Tsukuba, Japan) with the α_3 doughnut-like quaternary structure. The structure of $Oxy_{red/red}$:CAR shows CAR binds at the active site in such a conformation that the carbon atoms at the angular (C9a) and its adjacent (C1) are exposed to attack by O_2, and is stabilized by hydrogen bonding of the imino nitrogen with the carbonyl oxygen of G178. Binding of planar CAR at the active site causes the large movement of residues L202-T214 and D229-V238 towards the entrance of the catalytic pocket, especially the significant shifts of residues F204 and I231, resulting in the closure of the catalytic pocket to trap CAR inside.

In pathway 2, the crystals of $Oxy_{red/red}$ were moved out of the anaerobic chamber and exposed to pure O_2 for 5 min to obtain the O_2-bound Oxy (4b). The structure, determined at 2.2 Å resolution in Photon Factory, reveals that in absence of substrate, dioxygen binds skewed side-on to the active site, causing no significant conformational changes in the overall structure, compared with $Oxy_{red/red}$, except for the flip of some side chains

such as those of E233 and H234. Still, the catalytic pocket keeps open widely.

When both substrate and O_2 are available to the active site, substrate transformation starts. To obtain the substrate plus O_2-bound structure, crystals of $Oxy_{red/red}$:CAR were moved out of the anaerobic chamber and exposed to pure oxygen for 5 min before freezing. The structure determined at a resolution of 2.2 Å in Spring-8 shows different geometries in active sites A, B and C. Subunit A shows a positive density in the active site, which could not be modeled as planar CAR and individual dioxygen. Instead, the continuous electron density from the active site iron to the slightly puckered CAR suggests the presence of a covalent link between the iron and substrate. This suggests a presumed tricyclic alkylperoxo intermediate binds at the active site A ($Oxy_{ox/ox}$:CAR:O_2; (5)), which was generated during the hydroxylation reaction. The tricyclic moiety of alkylperoxo intermediate is still stabilized by G178 and the peroxo moiety is stabilized with the 2-His-1-carboxylate facial triad motif. Furthermore, the formation of alkylperoxo intermediate initiates the opening of the previously well-closed catalytic pocket caused the binding of substrate. The continuous and distorted ligand density in the active sites B and C and the disappearance of electron density of former 5-membered CAR ring indicates the cleavage of O-O bond of the peroxo moiety and the ring fission between C9a and N9 to form ABP-diol ($Oxy_{ox/ox}$:ABP-diol, (6)). The product remains bound at the active site with both oxygen atoms coordinated to the iron in an average distance of 2.2 Å. Generation of ABP-diol has resulted in wide re-opening of the catalytic pocket by movements of residues L202-T214 and D229-V238 (especially F204 and I231) back to the initial positions, through which the product is ready to be released from the active site.

Chapter 3. Product release from the active site of Oxy in CARDO

To understand the mechanism of product release in CARDO, commercially available biphenyl-2,2',3-triol (BP-triol) and biphenyl-2,3-diol (BP-diol) were used as products instead of ABP-diol in the soaking experiments to obtain the product-bound structures. The previously obtained crystals of $Oxy_{ox/red}$ (1) and $Oxy_{ox/red}$:Fd_{ox} complex (8b) were soaked in the DMSO solution of BP-triol or BP-diol for 5~10 min before cryo-cooling. The X-ray diffraction data were collected in Photon Factory.

The determined structure of BP-diol bound $Oxy_{ox/red}$:Fd_{ox} complex (7) at a resolution of 2.0 Å, consists of one molecule of Oxy and three Fd molecules, and the asymmetric unit of the crystal contains one $Oxy_{ox/red}$:Fd_{ox} molecule. BP-diol with low occupancy binds at active site A with both O atoms coordinated to Fe(II), which is similar with the binding mode of ABP-diol to Fe(III) mentioned above. While the two hydroxyl groups of BP-diol in active sites B and C have rotated away from Fe(II), resulting in a water molecule lying between the Fe(II) and proximal ring of BP-diol, significantly different with that of ABP-diol at the non-heme Fe(III). Compared with $Oxy_{ox/ox}$:ABP-diol, some conformational changes have been observed at the boundary of Oxy and Fd. For example, side chains of R11, K13 and R118 of Oxy have flipped to form interactions with residues in Fd to stabilize the complex of Oxy and Fd.

In pathway 3 for the product release, Fd_{ox} dissociates from $Oxy_{ox/red}$:product complex followed by the release of product. To get the product-bound $Oxy_{ox/red}$ in the absence of Fd_{ox} (8a), crystals of $Oxy_{ox/red}$ (1) were soaked with BP-triol or BP-diol solution for 5-10 min. The determined structure of $Oxy_{ox/red}$:BP-triol at a resolution of 2.3 Å reveals that this product binds at the active site with two hydroxyl groups coordinated to the iron, while the third hydroxyl group in the distal ring is stabilized by hydrogen bonds with G178 (3.4 Å) and two water molecules. While the structure of $Oxy_{ox/red}$:BP-diol determined at a resolution of 1.9 Å shows that this product analog binds at the active site through a water molecule at 1.8 Å from the Fe(II), which is similar with the binding mode of BP-diol in active sites B and C of $Oxy_{ox/red}$:Fd_{ox}:BP-diol. No obvious conformational changes are caused by the binding of BP-triol and BP-diol to the active site, except for the binding modes of BP-triol and BP-diol as described previously. Upon dissociation of Fd_{ox} from product-bound $Oxy_{ox/red}$,

interactions that stabilize Oxy:Fd complex are disrupted by the flip of side chains of related residues, including R11, K13 and R118 in Oxy. Then the subsequent release of BP-triol or BP-diol has caused a shift of residues A259-D261 towards the entrance of the catalytic pocket up to 1.3 Å (N260), leading to contraction of the entrance of the catalytic pocket.

In the pathway 4, *cis*-dihydrodiol product is released from the active site before the dissociation of $Oxy_{ox/red}$:Fd_{ox} complex. Comparison of $Oxy_{ox/red}$:Fd_{ox}:BP-diol and previously determined product-free $Oxy_{ox/red}$:Fd_{ox} (8b) shows that when the product is released from the active site, entrance of catalytic pocket is contracted caused by the movement of residues A259-D261, which is similar to the contraction caused by the product release from $Oxy_{ox/red}$.

Conclusions

On the basis of the series of Oxy structures bound with substrate, dioxygen, intermediate and products identified in this study, as well as those previously determined structures of Oxy and Fd in single and complex states, the mechanism of angular dioxygenation in CARDO has been elucidated (Fig. 2). (I) In the resting state, the mononuclear Fe(II) of $Oxy_{ox/red}$ has a distorted pentahedral geometry. Fe(II) is accessible easily for the solvent and substrate through a largely open catalytic pocket. (II) Fd_{red} transports an electron to the resting Oxy. (III) The obtained $Oxy_{red/red}$ shows a distorted octahedral coordination including two water molecules at the active site. The catalytic pocket opens widely. (IV) Coupling with reduced Rieske center, both substrate and O_2 are possible to bind to the Fe(II). (IVa) Accessibility of planar CAR to the active site results in the closure of the catalytic pocket by shifts of residues L202-T214 and D229-V238, especially F204 and I231 to trap the substrate inside; (IVb) while dioxygen bound to the substrate-free active site in a skewed side-on fashion has barely effects on the overall structure. (V) Availability of both substrate and dioxygen to the active site results in the formation of alkyloperoxo intermediate, accompanied by the partial opening of catalytic pocket. (VI) The alkylperoxo intermediate is converted to the *cis*-dihydrodiol product, with two O atoms coordinated to the non-heme Fe(III), resulting in the wide re-open of the pocket. (VII) The protonated bicyclic product with high flexibility is released from the re-reduced non-heme Fe(II). Oxy returns back to the resting state to start next turnover.

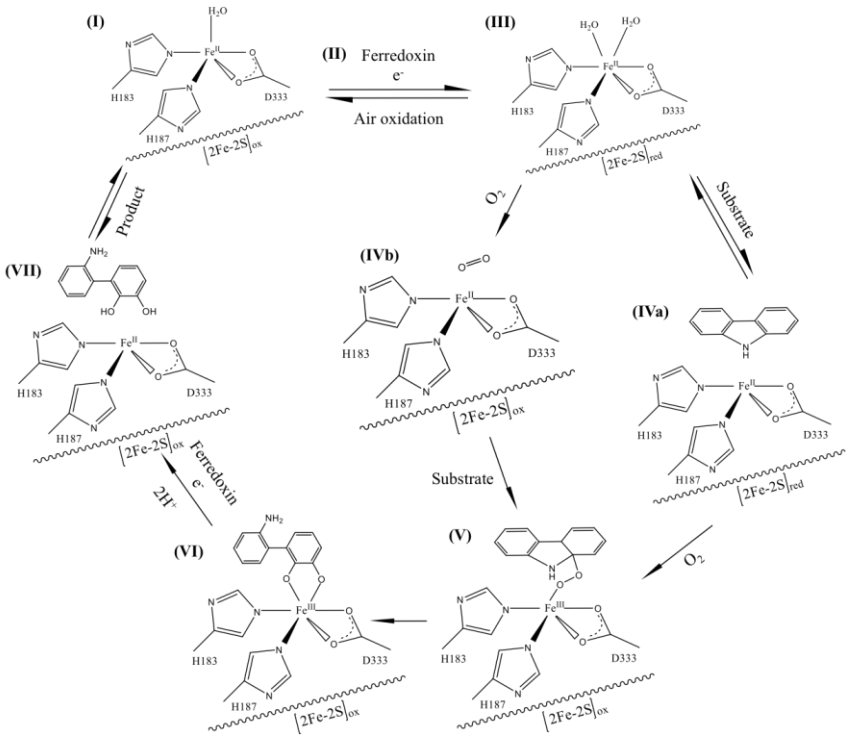

Fig. 2 Proposed mechanism of angular dioxygenation in CARDO. [2Fe-2S] refers to Rieske iron-sulfur cluster in the neighboring subunit.